

A Study of the Design and Development of A Versatile Polishing Machine for the Fabrication of Optical Fiber Probe for Medical Application

Y.C. Tsai^{1*}, G.M. Huang², J.H. Chen², M.C. Hsieh², S.W. Chen¹, J.A. Syu¹, I.C. Her²

¹Department of Mechanical Engineering, Cheng Shiu University, Kaohsiung, Taiwan, R.O.C.

²Department of Mechanical & Electro-Mechanical Engineering, National Sun Yat-Sen University, Kaohsiung, Taiwan, R.O.C.

Abstract: A versatile polishing machine (VPM) for the fabrication of optical fiber probe for medical application is designed and developed in this study. The VPM can keep the end-face of fiber at a fixed virtual pole of the fiber holder and abrasive pad. It is difficult for the commercially available optical fiber polishing machine to carry out such function. Five mechanisms have been proposed and the Quality Function Deployment method is adopted to evaluate the proposed five mechanisms. The Circular Motion Guide Mechanism is finally selected as the kinetic mechanism. In order to increase the fabrication reliability, a polishing turntable has been developed with a run-out smaller than $1\mu\text{m}$ at the polishing area. The double-variable curvature end-faces (DVCE) of optical fibers can be fabricated by controlling the fabricating parameters of the VPM, inclined angle, rotation angle and vertical displacement simultaneously. The DVCE has been fabricated with the concentricity less than $1\mu\text{m}$ between core and end-face. Optical fiber probes produced by the VPM are useful for the medical applications.

[Y.C. Tsai, G.M. Huang, J.H. Chen, M.C. Hsieh, S.W. Chen, J.A. Syu, I.C. Her. A Study of the Design and Development of A Versatile Polishing Machine for the Fabrication of Optical Fiber Probe for Medical Application. *Life Sci J* 2016;13(11):68-75]. ISSN: 1097-8135 (Print) / ISSN: 2372-613X (Online). <http://www.lifesciencesite.com>. 11. doi:[10.7537/marslsj131116.11](https://doi.org/10.7537/marslsj131116.11).

Keywords Mechanism Design, Polishing Machine, Optical Fiber, Micro End-face, Medical Probe

1. Introduction

Optical fibers provide convenient, safe, effective, and low-cost way to transfer and gather information or energy via light. Optical fibers can be used at delivering signals, communication, monitoring, and laser beam processing.

Alavi et al. used MRR to generate and trap chaotic signals along optical fiber to communication [1]. Zyaei et al. used asymmetric quantum well structure to be the optical switch that caused a sharp absorption or transparency in this visible optical probe [2]. Alsaidi et al. used optical fiber as sensors to detect partial discharge on natural palm oil [3]. Kao and Hockham demonstrated the optical fiber was a good wave guide for communication [4]. Ding et al. applied the wave-guided resonance optical element on GMR biosensor to detect DNA [5]. Balamurugan and Thanushkodi used optical fiber on the wind turbine blade to monitor the wind speed and density for blade adjustment [6]. Stock et al. compared different focusing fiber tips for improved oral diode laser surgery [7]. Royston et al. introduced the optical properties of fiber optic surgical tips [8] as shown in Figure 1. Tearney et al. used scanning single-mode fiber optic catheter-endoscope for topical coherence tomography [9] as shown in Figure 2.

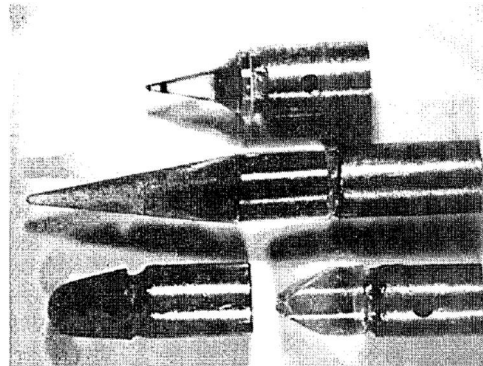


Figure 1. Various surgical tips [8]

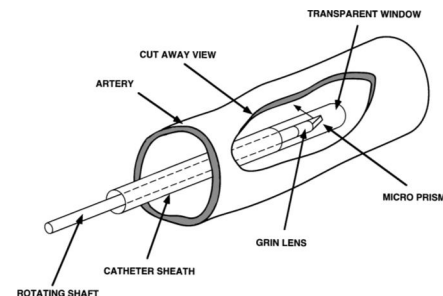


Figure 2. The OCT catheter-endoscope [9]

There exist many fabrication methods used to create optical fiber probes including laser micromachining [10-11], focused ion beam milling [12-13], chemical etching [14-16], and mechanical

polishing [17-24]. The mechanical polishing method, however, offers several advantages including reasonable accuracy, the possibility of fabricating different types of probes, and production scalability. For these reasons, the mechanical polishing method is one of the most popular optical probes fabrication processes.

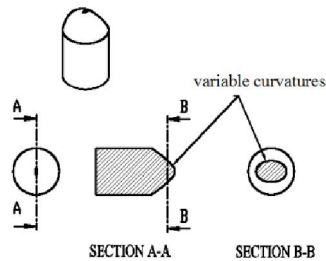


Figure 3. The double-variable curvatures probe

In this study, a special lapping machine should be developed with the aim of keeping the end-face of the optical fiber at the virtual pole. As such, it should keep the end-face of the optical fiber at a stationary area on the polishing pad while the optical fiber inclined angle θ varies. This special lapping machine would help producing various types of probes directly on the tips of optical fibers. Even the double-variable-curvature probe would be fabricated. As shown in figure 3. Using this special lapping machine, the offset between the probe and core of optical fiber would reduce to within $1\mu\text{m}$, which helps increasing the coupling efficiency.

2. Mechanism design

Double-variable curvatures can be fabricated by controlling the θ -, ϕ -, and H-axes simultaneously. The tip of the optical fiber should remain at a fixed position (a virtual pole) on the abrasive pad while the inclined angle varies. The fiber holder, kinetic mechanism, and the low run-out polishing turntable are introduced below.

2.1 The fiber holder and kinetic mechanism

For the fabrication of a double-variable curvature probe, the kinetic mechanism should generate the corresponding polishing path. This means that the inclined angle will be changed according to the variation of the probe curvature, while maintaining the probe of the fiber at the same height on the polishing table.

Drawing from mechanism design experience and brainstorming, there are five mechanisms that fit these requirements: (1) Coupler Cognate Mechanism, (2) Dressing Machine, (3) Pantograph Mechanism, (4) Straight-Line Generator Mechanism, and (5) Circular Motion Guide Mechanism, as shown in table 1.

Table 1. Kinetic mechanisms for the fiber holder

Drawing of Mechanism	CAD Model
<p>Coupler Cognate Mechanism</p>	
<p>Dressing Machine</p>	
<p>Pantograph Mechanism</p>	
<p>Straight-Line Generator Mechanism</p>	
<p>Circular Motion Guide Mechanism</p>	

Each of the five mechanisms presents their own advantages. In order to determine the most suitable fiber holder kinetic mechanism, the Quality Function Deployment (QFD) method [25] is adopted to quantify the performance of each mechanism into engineering specifications. First, five items are chosen as the index factors: (A) position repeatability; (B) simplicity of mechanism (which affects manufacture and assembly); (C) stability of the fiber during polishing; (D) ease of observation (should the microscope move while the mechanism is moving); and (E) ease of adjustment. Secondly, the five items

are compared with one another to determine the weighting of each item, as shown in table 2. Third, a grading table is created, as shown in table 3, to evaluate the performance functions of the five mechanisms. Finally, a matrix of product attributes against engineering characteristics is shown in table 4. Using this analysis, it is evident that the Circular Motion Guide Mechanism is superior to the other four mechanisms; therefore, the Circular Motion Guide Mechanism is chosen to be the kinetic mechanism of the fiber holder, and is shown in Figure 4.

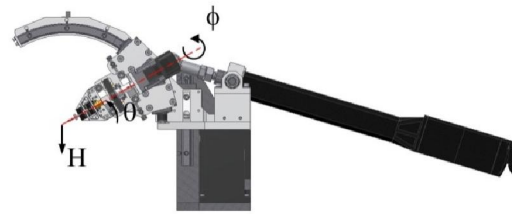


Figure 4. Three independent axes to fabricate double-variable curvature probes

Table 2. Weighting of each item

	A	B	C	D	E	Subtotal	Weighting
Position Repeatability	—	1	0	1	1	3	0.3
Ease of Configuration	0	—	0	1	0	1	0.1
Stability of Fiber	1	1	—	1	1	4	0.4
Ease of Observation	0	0	0	—	1	1	0.1
Ease of Adjustment	0	1	0	0	—	1	0.1
Grand Total						10	1.0

Table 3. Grading table

Grading	1	2	3	4	5
Levels	Bad	Poor	Normal	Good	Excellent

Table 4. Comparison results of the five mechanisms

	A	B	C	D	E	Amount
Weighting	0.3	0.1	0.4	0.1	0.1	1.0
Coupler Cognate Mechanism	4	1	4	5	1	3.5
Dressing Machine	4	4	4	5	3	4
Pantograph Mechanism	3	3	3	2	3	2.8
Straight-Line Generator Mechanism	2	4	3	2	4	2.8
Circular Motion Guide Mechanism	4	5	5	5	4	4.6

2.2 Low run-out polishing turntable

The contacting force of the optical fiber will change with the variation of the polishing turntable run-out, as shown in Figure 5. Considering the specifications of the commercial polishing machine and the results of our experiments, the end-face geometry is difficult to control and the fiber may be broken if the variation of the polishing turntable run-out is larger than 5µm. Since the commercial polishing turntable is expensive and not sold by itself, our research group has decided to design and develop a new polishing turntable.

The maximum allowable run-out of the turntable is ±5 µm, and the recommended run-out of the turntable is set as ±2.5 µm in our design for reliability. Figure 6 shows the 3D model of the turntable.

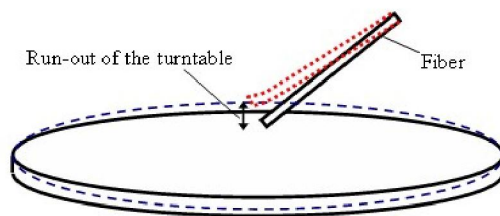


Figure 5. Diagram of the polishing turntable

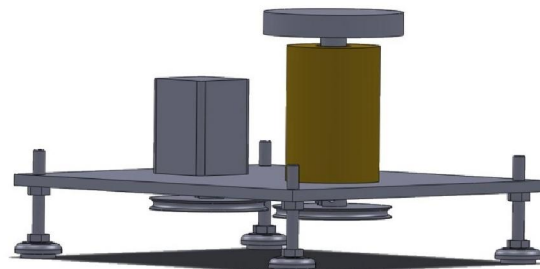


Figure 6. 3D model of the fiber lens polisher turntable

One of the main factors that affect the turntable run-out is the radial clearance of the bearing. A suitable length spindle shaft is designed to fit the design criterion of $\pm 2.5\mu\text{m}$. It is assumed that the turntable is a rigid body and that the dimensional accuracy is perfect. Here, a P5 grade bearing is chosen with a $0\sim 4\mu\text{m}$ radial run-out clearance of the inner ring. A maximum clearance of $4\mu\text{m}$ is chosen as our design criterion for reliability. Figure 7 is a sketch of the turntable and bearings.

Assuming D is the diameter of turntable and P is the length of the spindle shaft, then

$$\theta = \sin^{-1}\left(\frac{4\mu\text{m}}{P}\right) \quad (1)$$

$$\frac{D}{2} \sin \theta \leq 2.5\mu\text{m} \quad (2)$$

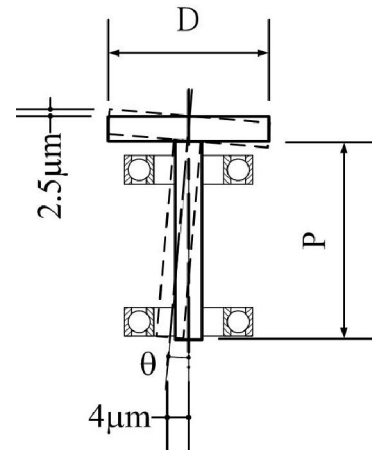


Figure 7. Sketch of turntable and bearings

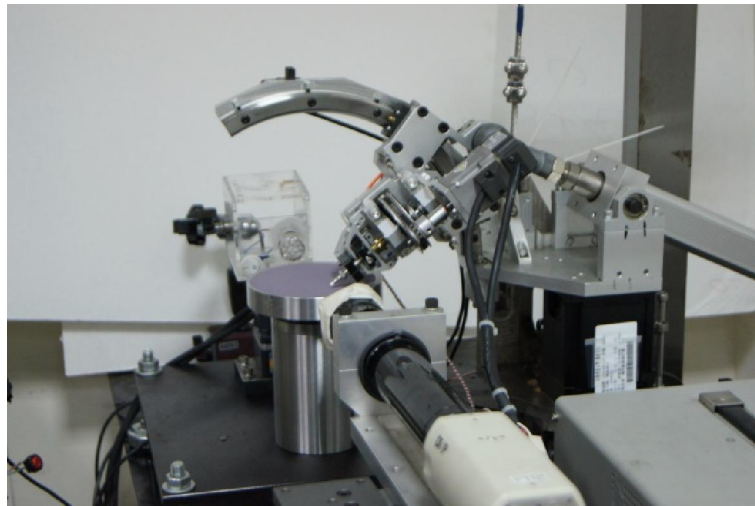


Figure 8. Photograph of the versatile polishing machine

Equation (1) shows that increasing the shaft length reduces the inclined angle θ , and a smaller θ helps reduce the turntable run-out. However, the length of the spindle shaft should be limited since a longer shaft length results in lower machining accuracies of the spindle shaft and the turntable. The length of the spindle shaft is determined to be 120 mm.

The diameter of the turntable should be as small as possible since a larger diameter will cause a higher run-out. The diameter, D , of the turntable is set at 120 mm, because it should be larger than the diameter of the diamond polishing pad (110 mm). The versatile polishing machine (VPM) is shown in Figure 8.

3. Experiments and Polishing results

3.1 Preparation of experiments

Since the mechanism is designed to grind objects

with a tolerance of only several microns, the polishing conditions will have a large effect on the results. The preparation of experiments is introduced below.

Tool Preparation:

- (1) Polishing machine: the versatile polishing machine.
- (2) Polishing film: 3M Diamond Lapping film 661X with 1 μm grade.
- (3) Polishing material: glass single mode optical fiber, Fujikura FutureGuide® LWP.
- (4) Slurry: no slurry.

Preprocessing Steps:

- (1) Clean the turntable with alcohol.
- (2) Place polishing film on the turntable with a small amount of water between them. Squeeze excess water and air with a plastic ruler; this will keep the polishing film stuck on the turntable.
- (3) Cut the single mode optical fiber to a length

in the range 15-20 cm. The jacket and buffer should be stripped at one end to leave 30 mm exposed. Clean the stripped optical fiber with alcohol.

(4) Cut the stripped optical fiber using a fiber cleaver, leaving a 12 mm length.

(5) Adjust the H-axis until the virtual pole stays on the turntable. Set the θ -axis of the fiber holder, to 90° . Put the optical fiber through the fiber holder until the stripped end touches the turntable. This will help keep the length L_0 , from the ferrule to the end of the optical fiber, constant. The length is set to be 1.8 mm.

(6) Adjust the CCD microscope to a suitable magnification.

(7) Check that the end of the optical fiber will withstand tension without bending due to the polishing force, as shown in Figure 9. The distance is set to be 30 mm from the center point.

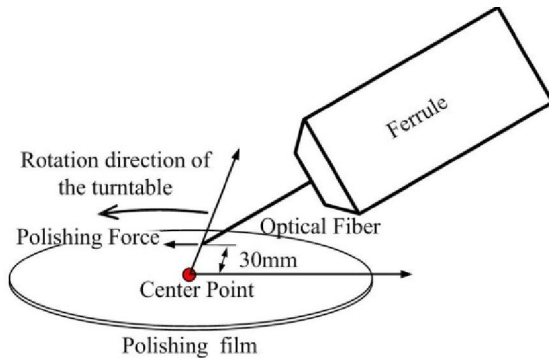


Figure 9. Schematic drawing of the optical fiber on the polishing film

The tool preparation and preprocessing steps detailed above help to reduce variations in the polishing results under constant polishing parameters.

3.2 Polishing parameters and results

In this study, the Preston equation [26] is used as the governing equation for the polishing operation. The Material Removal Rate (MRR) can be expressed as follows:

$$\frac{dH}{dt} = R_H = K \frac{N}{A} V \tag{3}$$

where K is the Preston coefficient ($\mu\text{m}^2/\text{mN}$), R_H is the thickness removal rate ($\mu\text{m/s}$), N is the contacting force (mN), A is the polishing area (μm^2), and V is the polishing velocity ($\mu\text{m/s}$).

Since the Preston equation is derived from plate glass polishing, equation (3) should be modified if the polishing area varies with time.

Since $dQ=AdH$, the MRR is modified as follows:

$$\frac{dQ}{dt} = R_Q = KNV \tag{4}$$

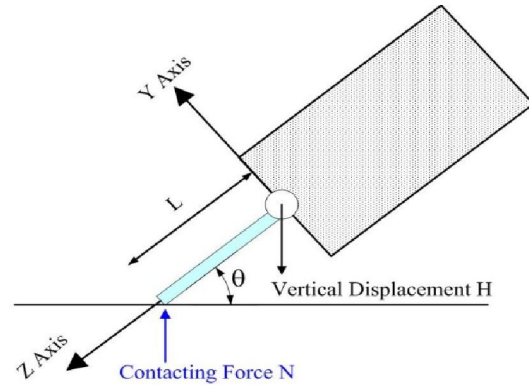


Figure 10. Free body diagram of the polishing process

where R_Q is the volume removal rate ($\mu\text{m}^3/\text{s}$). From equation (4), the volume removal rate R_Q is proportional to polishing velocity, V , and contacting force, N . The polishing velocity is determined by setting the speed of the abrasive pad and work piece, and is held constant during the polishing operation. The contacting force is determined by the position control. The contacting force may be varied during polishing, and its value is derived from beam theory. Figure 10 shows the free body diagram for the position control model with the contacting force determined from beam theory.

From beam theory, the position control mode equations are as follows:

$$EIy(z) = \frac{N \cos \theta}{6} (-z^3 + 3Lz^2) \tag{5}$$

$$EI\hat{\theta}(z) = \frac{N \cos \theta}{2} (-z^2 + 2Lz) \tag{6}$$

$$M(z) = N \cos \theta (L - z) \tag{7}$$

The relationship between deflection, $y(z)$, and vertical displacement, $H(t)$ is as follows:

$$y(L) = H(t) / \cos \theta \tag{8}$$

$$H(t) = H_0 - H_R(t) \tag{9}$$

Where H_0 is the initial vertical displacement and $H_R(t)$ is the removed thickness.

Combining equations (5), (8), and (9), the contacting force can be calculated if the vertical displacement is known:

$$N = \frac{3EI(H_0 - H_R)}{L^3 \cos^2 \theta} \tag{11}$$

From Eq. (3), the material removal rate is proportional to the contacting force N . In the position control mode, the contacting force is proportional to the vertical displacement $H(t)$ as shown in Eq. (11). The polishing parameters can be set as shown in Figure 11. Considering the H-axis and ϕ -axis as polar

coordinates, a_i and b_i represent different vertical displacements at different ϕ angles at the i^{th} polishing contour.

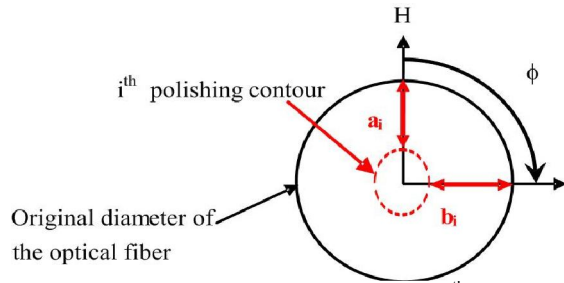


Figure 11. Polishing parameter at the i^{th} polishing contour

To achieve continuous double-variable curvatures, all three axes (θ , ϕ , and H) must work simultaneously. The parameters are defined in Microsoft Excel and are imported into LabView® as shown in Table 5.

Table 5. Polishing parameters of continuous double-variable curvatures

Inclined angle (degree)	Rotation angle (degree)	Vertical displacement H (mm)	Turntable speed (rpm)
30-60	0-360	0-40	200

Figure 12 shows the elliptical end-face probe. Figure 13 shows the double-variable curvatures probe that is produced by arc discharging the polished elliptical end-face probe [27]. The VPM developed in this study can not only fabricate double-variable curvatures, but can also fabricate other kinds of end-faces, as shown in Figures 14, 15, 16, and 17.

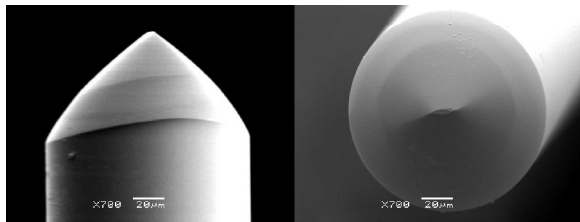


Figure 12. Elliptical end-face probe

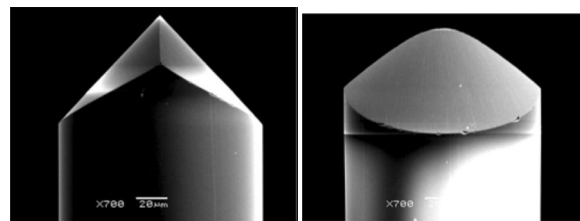


Figure 13. Double-variable curvature probe [27]

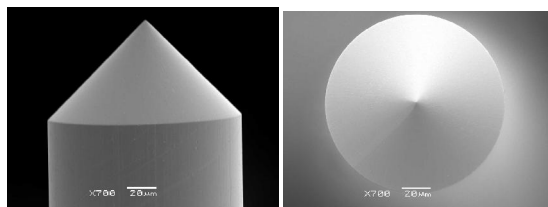


Figure 14. Cone-type end-face probe

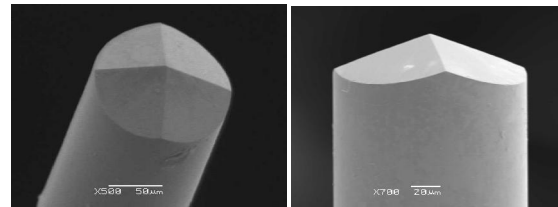


Figure 15. Pyramid-type end-face probe

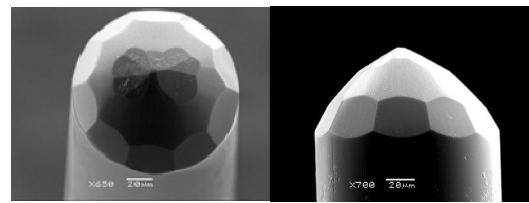


Figure 16. Polygonal hemispherical end-face probe

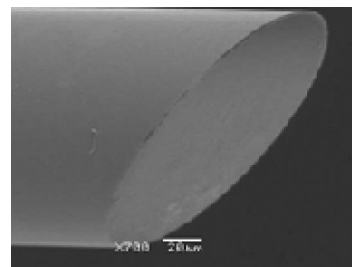


Figure 17. Bevel end-face probe

4. Conclusions

In this study, a polishing machine is designed and developed to fabricate probes with medical applications. The kinetic mechanism for the VPM is a Circular Motion Guide Mechanism, which was selected by using the Quality Function Deployment (QFD) method. The VPM has five axes: the spinning axis ϕ , rotation axis θ , vertical axis H , electric torque control axis α , and the polishing turntable. The VPM

is able to rotate about a fixed virtual pole during the polishing operation. A low run-out polishing turntable is also designed and developed in this study, with a maximum run-out of about $\pm 2 \mu\text{m}$ at the polishing position. The low run-out turntable helps to ensure that the contacting force does not vary significantly during the polishing operation. The double-variable curvatures end-face (DVCE) has been fabricated with the concentricity less than $1 \mu\text{m}$ between core and end-face [27].

The VPM developed herein can be used to fabricate many types of probes, including the cone-type, pyramid-type, bevels, the polygon hemisphere-type, and double-variable curvature. These have respective potential applications as a laser beam wave guide for surgical application [8], as a mirror to inspect tissue [9], a base for growing a nanotube probe [28], as a nanoindenter probe [29], as a mirror to measure displacement on the order of micrometers [30], as a probe to measure the displacement for high speed tribological measurement [31], and to increase the coupling efficiency to as much as 88% [27]. A R.O.C. Patent, I378010, has been filed.

5. Acknowledgment

This work was supported by the National Science Council, R.O.C., under contracts NSC-96-2221-E-230-016, NSC-96-2221-E-230-017, NSC-97-2221-E-230-010, and NSC-97-2221-E-230-011.

References

- Alavi S.E., Amiri, I.S., Idrus, S.M., Supa'at, ASM., Ali, J., Chaotic signal generation and trapping using an optical transmission link, *Life Science Journal*, 2013, 10(9s):182-196.
- Zyaei M., Faraji Sarir M., and Rahmani A., Quantum well terahertz switch based on electromagnetically induced transparency, *Life Science Journal*, 2013, 10(6s):292-294.
- Kharkwal, G., Mehrotra, P., Rawat, Y.S., Comparison study of sensitivity between three sensors to detect partial discharge on natural palm oil, *Life Science Journal*, 2013, 10(4):369-372.
- Kao, K.C., Hockham, G.A., Dielectric-fibre surface waveguides for optical frequencies. *Proc. IEE.*, 1966, 113(7):1151-1158.
- Ding, T.J., Lue, J.H., Tsai, Y.L., Tsung-Hsun Yang, T.H., Chang, J.Y., Chen, W.Y., Monitoring DNA hybridization with a simply manufactured GMR biosensor, *Life Science Journal* 2012, 9(2):1015-1019.
- Balamurugan, P.S. and Thanushkodi, K., Effective p-hit methodologies for generation monitoring system, *Life Science Journal*, 2013, 10(2):2981-2986.
- Stock, K., Stegmayer, T., Graser, R., and Forster, W., Cline, Comparison of different focusing fiber tips for improved oral diode laser surgery, *lasers in surgery and medicine*, 2012, 44(10): 815-823.
- Royston, D., Waynant, R., Banks A., Ramee, S., and White C.J., Optical properties of fiber optic surgical tips, *Applied optics*, 1989, 28(4):799-803.
- Tearney, G.J., Boppart, S.A., and Bouma, B.E., Scanning single-mode fiber optic catheter-endoscope for optical coherence tomography, *Optics letters*, 1996, 21(7): 543-545.
- Presby, H.M., Benner, A.F., and Edwards, C.A., Laser Micromachining of Efficient Fiber Microlenses, *Applied Optics*, 1990, 29(18): 2692-2695.
- Presby, H.M. and Giles, C.R., Asymmetric Fiber Microlenses for Efficient Coupling to Elliptical Laser Beams, *IEEE Photonics Technology Letters*, 1993, 5(2):184-186.
- Fu, Y.Q., Ngoi, K.A., and Ong, N.S., Diffractive Optical Elements with Continuous Relief Fabricated by Focused Ion Beam for Monomode Fiber Coupling, *Optics Express*, 2000, 7(3):141-147.
- Schiappellia, F., Kumar, R., Prasciolua, M., Cojoca, D., Cabrinia, S., Vittoriob, M.D., Visimbergab, G., Gerardinoc, A., Degiorgiod, V. and Fabrizioa, E.D., Efficient Fiber-to-Waveguide Coupling by a Lens on the End of the Optical Fiber Fabricated by Focused Ion Beam Milling, *Microelectronic Engineering*, 2004, 73-74:397-404.
- Pan, J.J., Arnold, M.P., and Barton, J.C., "Micro Lens Formation at Optical Fiber Ends", United States Patent Disclosure 4118270 (1978).
- Ghafoori-Shiraz, H. and Asano, T., Microlens for Coupling a Semiconductor Laser to a Single-Mode Fiber, *Optics Letters*, 1986, 11(8):537-539.
- Wong, P.K., Wang, T.H., and Ho, C.M., Optical Fiber Tip Fabricated by Surface Tension Controlled Etching, *Proceedings of Solid-State Sensor, Actuator and Microsystems Workshop*, Hilton Head Island, South Carolina, USA, 2002, 94(7):94-97.
- Shah, V.S., Curtis, L., Vodhanel, R.S., Bour, D.P., and Yang, W.C., Efficient Power Coupling From a 980-nm, Broad-area Laser to a Singlemode Fiber Using a Wedge-Shaped Fiber Endface, *Journal of Lightwave Technology*, 1990, 8(9):1313-1318.

18. Modavis, R.A. and Webb, T.W., Anamorphic Microlens for Laser Diode to Single-Mode Fiber Coupling, *IEEE Photonics Technology Letters*, 1995, 7(7):798–800.
19. Yoda, H. and Shiraishi, K., A New Scheme of a Lensed Fiber Employing a Wedge-Shaped Graded-Index Fiber Tip for the Coupling between High-Power Laser Diodes and Single-Mode Fiber, *Journal of Lightwave Technology*, 2001, 19(12):1910-1917.
20. Yoda, H. and Shiraishi, K., Cascaded GI-Fiber Chips with a Wedge Shaped End for the Coupling between an SMF and a High-Power LD with Large Astigmatism, *Journal of Lightwave Technology*, 2002, 20(8):1545–1548.
21. Yeh, S.M., Lu, Y.K., Huang, S.Y., Lin, H.H., Hsieh, C.H. and Cheng, W.H., A Novel Scheme of Lensed Fiber Employing a Quadrangular-Pyramid-Shaped Fiber Endface for Coupling between High-Power Laser Diodes and Single-Mode Fibers, *Journal of Lightwave Technology*, 2004, 22(5):1374-1379.
22. Yeh, S.M., Huang, S.Y., Hsieh, C.H. and Cheng, W.H., A New Scheme of Conical-Wedge-Shaped Fiber Endface for Coupling Between High-Power Laser Diodes and Single-Mode Fibers, *Journal of Lightwave Technology*, 2005, 23(4):1781-1786.
23. Lu, Y.K., Tsai, Y.C., Liu, Y.D., Yeh, S.M., Lin, C.C., and Cheng, W.H., Asymmetric Elliptic-Cone-Shaped Microlens for Efficient Coupling to High-Power Laser Diodes, *Optics Express*, 2007, 15(4):1434-1442.
24. Tsai, Y.C., Liu, Y.D., Cao, C.L., Lu, Y.K. and Cheng, W.H., A New Scheme of Fiber End-Face Fabrication Employing a Variable Torque Technique, *Journal of Micromechanics and Microengineering*, 2008, 18(5), 055003, doi:10.1088/0960-1317/18/5/055003.
25. Cross N, Engineering design methods strategies for product design, (2002), p.108, John Wiley & Sons. New York.
26. Preston F.W., The theory and design of plate glass polishing machines, *Journal of the Society of Glass Technology*, 1927, 11:214-256.
27. Liu Y.D., Tsai Y.C., Lu Y.K., Wang L.J., Hsieh M.C., Yeh S.M. and Cheng, W.H., New Scheme of Double-Variable-Curvature Microlens for Efficient Coupling High-Power Lasers to Single-Mode Fibers, *Journal of Lightwave Technology*, 2011, 29(6):898-904.
28. Akita S., Nishijima H., Nakayama Y., Tokimasa F. and Takeyasu K., Carbon nanotube tips for a scanning probe microscope: their fabrication and properties, *Journal of Physics D: Applied Physics*, 1999, 32(9):1044-1048.
29. Micro Star Technologies, “Nano indenter specifications”, available from <<http://www.microstartech.com/index/NANOINDENTERS.pdf>>, (accessed 2013-03-31).
30. Tsai, Y.C., Lin, W.R., Huang, G.M., Liu, Y.D., and Cheng, W.H., A Feasibility Study of the Measurement of the PWS of Butterfly-Type Laser Module Packages Employing Micro Polygon-Mirror and PSD, *International Journal of Automation and Smart Technology*, 2011, 1(2):101-109.
31. Itoh, S., Imai, K., Fukuzawa, K., Hamamoto, Y., Zhang, H., Displacement Measurement for High Speed Tribological Measurement Using Oscillating Optical Fiber Probe, *Journal of Advanced Mechanical Design, Systems, and Manufacturing*, 2010, 4(1):2-14.

11/25/2016